Local MP2 Study of Naphthalene, Indole, and 2,3-Benzofuran Dimers

Serguei Fomine,* Mikhail Tlenkopatchev, Sergio Martinez, and Lioudmila Fomina

Instituto de Investigaciones en Materiales, Universidad Nacional Autónoma de México, Apartado Postal 70-360, CU, Coyoacán, México DF 04510, Mexico

Received: November 30, 2001; In Final Form: February 1, 2002

The ground-state structures of the van der Waals dimers of naphthalene, indole, and 2,3-benzofuran have been optimized at the local MP2/6-31G* level of theory without any symmetry restrictions. The binding energies of complexes were evaluated at the local MP2 approximation using 6-31G*, 6-311G**, cc-pvtz(-f), and aug-pvtz(-f) basis sets. The binding energies are strongly dependent on the basis set size and not completely converged even for the largest basis set tested. The relative stability of studied complexes is, however, similar for the two largest basis sets used in this study. It was found that in all cases the major contribution to the binding energy is the correlation energy representing from 90 to 100% of all stabilization energy. Among two types of studied complexes, parallel and T-shaped, the parallel complexes are the most stable ones due to better correlation stabilization, with one of the naphthalene parallel dimers being the most stable out of all studied complexes showing the stabilization energy of −8.02 kcal/mol. All indole and T-shape 2,3-benzofuran dimers evidence N−H and C−H−π hydrogen bonds as follows from the geometry changes and the charge transfer from one molecule to another. The Kitaura−Morokuma analysis of SCF binding energy shows that T-shape complexes are better stabilized by electrostatic interactions and less destabilized by exchange repulsion compared to parallel ones.

Introduction

One of the major goals of chemistry in recent times has been the investigation and understanding of weak interactions.[1−6] Thus, aromatic−aromatic interactions play important roles in many chemical and biological systems. They control, among others, the base−base interactions leading to the double helical structure of DNA, the function of the special pair in photosynthetic reaction centers, the packing of aromatic crystals, the formation of aggregates, the binding affinities in host−guest chemistry, and the conformational preferences of polyaromatic macrocycles.

One of the major problems in the petroleum and natural gas industries is the deposition of condensed aromatic hydrocarbons and other heavy organic compounds existing in the crude oil which is directly linked with the interactions between aromatic molecules. The production, transportation, and conservation of petroleum can be significantly affected by deposition of associates from the aromatic hydrocarbon molecules and other heavy organics in the oil well, pumps, transfer pipelines, etc., with devastating economic consequences.

The molecular systems ideally suited for a detailed study of intermolecular potentials are the van der Waals (vdW) dimers and higher clusters of aromatic hydrocarbons and heterocycles. The simplest and most extensively studied aromatic cluster is the vdW dimer of benzene. On the basis of molecular beam electric resonance spectroscopy, which shows the benzene dimer to be a polar and an asymmetric rotor, Klemperer and coworkers[7,8] proposed a T-shaped geometry confirmed by ab initio calculations[9] at the CCSD(T)/aug-ccPVDZ//MP2/DZ+2P level.

Syage and Wessel[10] were the first to observe the vdW dimer of naphthalene in the mass-resolved resonant two-photonionization spectrum of seeded molecular beams of naphthalene, while Chakraborty and Lim[11] obtained evidence for the presence of two structurally different dimers of anthracene in a supersonic jet. The calculations performed by Gonzalez and Lim for naphthalene and anthracene dimers at the MP2/6-31+G//MP2/6-31G level of theory yield two low-energy conformers of very similar energies: D_{2d} (crossed) and C_{2h} (parallel-displaced). Conformers, analogous to the T-shaped dimer of benzene, are less stable than the crossed and the parallel-displaced dimers.[12] The authors also modeled trimers of naphthalene at the MP2/6-31+G//MP2/6-31G level.[13] The lowest-energy structure was found to be the edge-to-face cyclic (C_{3h}) geometry in which the three equivalent naphthalene moieties are arranged with their long in-plane axes parallel.

The studies of heterocyclic dimers were limited to a pyrrole dimer. The calculations at the MP2/6-31G** level reveal that the N−H hydrogen of one monomer points toward the ring plane of the other monomer with a distance 1.909 Å, which is a clear manifestation of hydrogen bond formation in this simple model of aromatic−aromatic interactions.[14]

As can be seen, the method most widely used to model intermolecular interactions which takes into account the effect of electron correlation at relatively low computational cost is the second-order Møller−Plesset (MP2) theory.[15] The accuracy of density functional theory (DFT) based methods, which allow one to include electron correlation at lower computational costs, depends to a large extent on how good are the functionals for the particular system under consideration. Moreover, DFT reproduces very poorly the dispersion interaction,[16] which is of primarily importance for weakly bound aromatic clusters. On the other hand, local correlation methods have recently emerged as alternatives for the study of intermolecular interactions. Reduced step dependence of the computational cost on the size of molecule and reduced basis set superposition error (BSSE) are two important advantages of the local MP2 method

* Corresponding author. E-mail: fomine@servidor.unam.mx.

10.1021/jp014375y CCC: $22.00
Published on Web 03/15/2002

(LMP2).[17] In particular, it has been shown that LMP2 and CP-corrected MP2 equilibrium geometries of water and water clusters are fairly close.[17,18] In this work we present the first results of molecular modeling for naphthalene, indole, and 2,3-benzofuran dimers using the local MP2 approach. These molecules are important components of crude oil.

Computational Details

All geometry optimizations were carried out with the Jaguar 4.1 program at the LMP2/6-31G* level in the gas phase[19] without any symmetry restrictions. Single point energies of studied molecules and complexes were calculated at the LMP2 level of theory using 6-311G**, cc-pvtz, and aug-cc-pvtz basis sets with f-functions removed. The last basis set will be referred to as cc-pvtz(-f). LMP2 is already designed to avoid BSSE; therefore, only the HF counterpoise correction term has been computed according to ref 20. MP2 NBO analysis and SCF energy partition analysis were carried out with the Gaussian 98[21] and GAMESS[22] suite of programs, respectively.

To test the applicability of the selected computational model the preliminary calculations on the benzene dimer molecules were carried out. Benzene forms two most stable dimers of almost similar energy: T-shaped and parallel displaced (PD).[9] To the best of our knowledge the highest treatment level used for this system is the partial optimization at the CCSD(T)/cc-pvdz level. According to these calculations the binding energies for T-shaped and PD-displaced benzene dimers were of −2.08 and −1.80 kcal mol, respectively. In our case dimers were optimized without any geometry restriction at the LMP2/6-31G* level and the binding energies were evaluated using 6-311G**, cc-pvdz, cc-pvtz(-f), and aug-cc-pvtz(-f) basis sets. The corresponding binding energies for T-shaped and PD dimers were −1.15, −1.16, −1.71, −2.46 and −0.47, −0.57, −1.60, −2.76 kcal/mol. As can be seen, the results of LMP2/cc-pvdz//LMP2/6-31G* and CCSD(T)/cc-pvdz// CCSD(T)/cc-pvdz are in very good agreement. Thus, LMP2 model predicts the T-dimer to be more stable than the PD one in agreement with the coupled cluster model. Moreover, LMP2 reproduces CCSD(T) dependence of the stabilization energies on the basis set. The energy gap between T-shaped and PD dimers decreases with the completeness of the basis set.

On the other hand, the conventional MP2 model strongly overestimates the stabilization energy and leads to an incorrect global minimum.[9] The initial geometries were obtained in two ways. For naphthalene dimers four structures **T1**, **T2**, **C**, and **PD** (Figure 1) were taken from ref 12, where low-energy conformers were found using the MM3 force field MD followed by MP2/6-31G level optimization. Unlike the case for ref 12, no symmetry restrictions were used for the geometry optimization. One more naphthalene dimer, two indole, and two 2,3-benzofuran dimers were located using the approach described by Gonzalez and Lim.[12] Molecular dynamics (MD) trajectories were computed with the molecular mechanics (MM2) force field, using the Chem 3D program. To determine the possible low-energy structures, a series of 100 ps MD simulations (after previous equilibration for 100 ps) were carried out at 150 K, starting with different geometries. In each simulation, a fixed time step of 4 fs was used, and only the lowest energy structures were selected. These geometries were further optimized with the MM2 force field using the Chem 3D program. The optimized geometries of the lowest-energy minima located using the MM2 force field were then used as the initial guess for additional MD simulations to search for extra minima. If an additional minimum was found, the process was repeated until no further minimum was located.

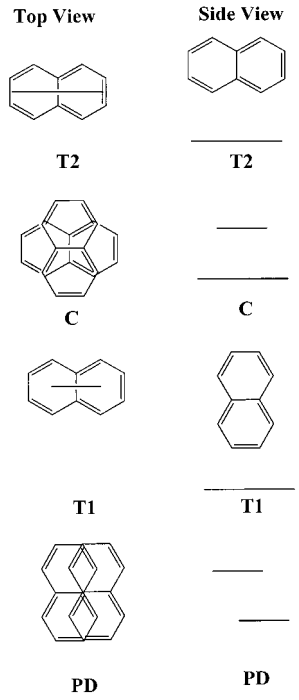

Figure 1. Naphthalene dimers studied by Gonzalez and Lim.[12]

Results and Discussion

Naphthalene Dimers. Naphthalene dimers were first studied by Gonzalez and Lim[12] at the MP2/6-31+G//MP2/6-31G level of theory where the four lowest energy conformers **T1**, **T2**, **C**, and **PD** (Figure 1) were located **T1**, **T2**, **C**, and **PD** (Figure 1) with the **PD** and **C** dimers found to be the most stable ones. However, the relatively small basis sets used in that study do not allow one to make clear conclusions not only about the absolute binding energies of different complexes but also about their relative stability. Another shortcoming is related with the symmetry restriction imposed on studied complexes. Thus, for the **T1**, **T2**, and **C** structures C_{2v} and C_{2h} symmetries were assumed, while it is known that the benzene T-dimer does not possess C_{2v} symmetry.[12] We tried to overcome these drawbacks in this study by improving the quality of basis sets for optimization and especially for the energy evaluation. In addition, no symmetry restrictions were imposed on complexes during their optimization. The optimized structures of naphthalene complexes are shown in Figure 2. As can be seen, the geometry of naphthalene complexes changes when symmetry restrictions are removed. While **PD** dimers maintain their geometry, **T1**, **T2**, and **C** complexes break their C_{2v} and C_{2h} symmetries on optimization. Naphthalene rings become tilted in T complexes, and in the case of the **C** dimer one naphthalene ring is displaced with the dihedral between C9−C10 bonds becoming 50.2° instead of 90° in the C_{2h} **C** dimer. The comparison can be made between the **PD** dimer[12] optimized at the MP2/6-31G level and the **PD1** complex optimized at the LMP2/6-31G* level. For this complex both models produce quite similar geometries. While in the MP2/6-31G-optimized structure the distance between naphthalene rings is of 3.5 Å, the LMP2/6-31G* model gives a looser complex with equilibrium distance between naphthalene planes of 3.64 Å. On the other hand, the relative displacements are almost the same for both models (1.54 and 1.52 Å for the MP2/6-31G and LMP2/

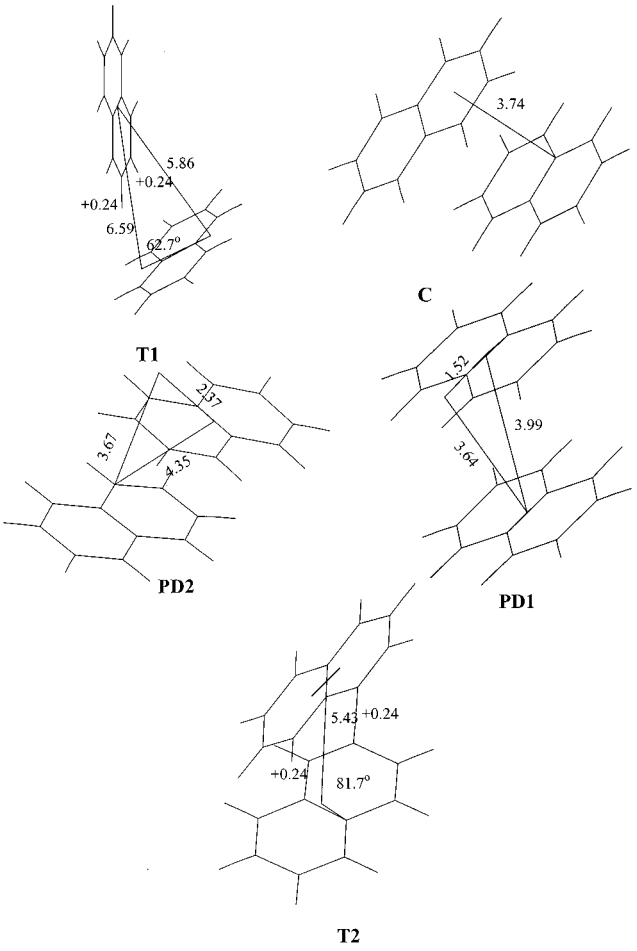

Figure 2. LMP2/6-31G*-optimized geometries of naphthalene complexes.

6-31G* levels, respectively). Table 4 shows LMP2 binding energies of the studied complexes. As can be seen, the completeness of the basis set affects not only the absolute but also the relative stability of the complexes. Large basis sets (cc-pvtz(-f) and aug-cc-pvtz(-f)) predict the **C** and **PD2** complexes to be the most stable, while smaller basis sets predict T-shaped complexes to have higher binding energies. It is noteworthy that a similar trend is observed for the MP2 model where the MP2/6-31G//MP2/6-31G model favors T-shaped dimers while MP2/6-31+G//MP2/6-31G calculations predict **PD** and **C** complexes to be the most stable structures.[12]

As can be seen in the analysis of Tables 3 and 4, where SCF and LMP2 binding energies are listed, the naphthalene complex stability is almost completely due to the correlation energy. All naphthalene complex binding energies calculated at the SCF level are positive or only slightly negative. In other words, electron correlation is responsible for the stability of naphthalene complexes. Table 5 shows the correlation energy contributions to the complex stability. As seen, this contribution increases strongly with basis set completeness for **PD** and **C** dimers, thus favoring their stability when large basis sets are used. In the case of **T** complexes, this increase is far less. Since dispersion interaction, which has an important contribution from correlation energy,[23] is a short range one, it decreases rapidly with distance. The average separation distances between atoms in **T** dimers are larger than those in **C** or **PD** complexes resulting in lesser dispersion stabilization for the former. This fact can explain the basis set dependence of stabilization energies for **T**, **PD**, and **C** naphthalene dimers. Since the correlation stabilization contributes more to **PD** and **C** dimers than to **T** ones, larger basis sets recover more correlation energy in the case of **PD** and **C** dimers favoring their stability. A similar trend is observed for **PD** and **T** benzene dimers[9] at the CCSD(T) level of theory. Another conclusion that can be made by analyzing Tables 3 and 4 is that BSSE becomes small (less than 0.5 kcal/mol) when the aug-cc-pvtz(-f) basis set is used, thus making unnecessary BSSE correction in the case of LMP2/aug-cc-pvtz(-f) calculations. The cc-pvtz(-f) basis set although producing larger BSSE still keeps it within 1 kcal/mol in most cases. On the other hand, smaller basis sets such as 6-311G** and especially 6-31G* generate BSSE comparable with binding energies; moreover, the relative stability of naphthalene dimers calculated with cc-pvtz(-f) or aug-cc-pvtz(-f) differs from that obtained by using smaller basis sets. Therefore, even in the case of the 6-311G** basis set care must be taken to estimate the relative stability of the vdW complexes.

As can be seen from the Table 3, the SCF binding energies of **T1** and **T2** complexes are far less positive compared to the **PD** and **C** ones which can be related to C−H−π interactions. The existence of such kinds of interactions has recently been demonstrated for a methane−benzene complex.[24] The formation of a conventional H-bond normally results in subtle shifts of the electron density.[25] Even though these shifts are relatively small in magnitude, they have been found to be useful in the identification of such bonds. This electron density is drawn not only from the lone pair of the acceptor molecule participating in the H-bond but from the entire molecule. Consequently, the density rather than being localized over a particular region delocalizes throughout the donor molecule. The NBO MP2/6-31G* analysis of electron density in the **T1** and **T2** complexes (Table 6) shows a subtle charge transfer from one naphthalene molecule to another thus suggesting the existence of a C−H−π interaction in T-shaped naphthalene complexes. The geometry of these complexes (C−H bond pointing to the center of aromatic rings) suggests $\pi-\sigma^*$ interaction between two naphthalene molecules. No geometrical changes is observed, however, in naphthalene molecules indicative of very weak character of the interactions if at all.

Indole Complexes. Unlike naphthalene, indole has a polar N−H bond and must be able of forming relatively strong π-facial hydrogen bonds similar to that observed in the pyrrole dimer.[14] Figure 3 shows the LMP2/6-31G*-optimized geometry of two most stable indole complexes. An important feature noted in the structure of the **C1** complex is the position of the N−H hydrogen relative to the molecular plane of indole. The H is directed to the ring plane of indole with a distance of 2.37 Å, indicating that the aromatic p-cloud acts as a hydrogen bond acceptor. The hydrogen bond involving an aromatic ring has been also found in other systems such as a water−benzene complex.[26]

The N−H bond length in the **C1** complex is 1.017 Å, while isolated indole molecule has an N−H bond length of 1.011 Å at the same level of theory. Similar increase of N−H bond length was observed for pyrrole dimers, confirming the π-facial hydrogen bond existence in the **C1** complex.[14] The NBO analysis of MP2/6-31G* density shows a slight decrease in bond order of N−H in **C1** compared to free indole from 0.966 to 0.962 together with stronger charge transfer (0.009 e, Table 6) from one indole molecule to another compared to **T1** and **T2** naphthalene complexes, which is an important indication of a π−hydrogen bond in the **C1** complex. Due to π−hydrogen bonds in the **C1** complex the SCF binding energies are negative. However, even in this case the major contribution to stabilization

TABLE 1: HF Energies (hartee) of Studied Molecules and Their van der Waals Complexes Calculated at LM2/6-31G* Geometries

molecule	6-31G*	6-311G**	cc-pvtz(-f)	aug-cc-pvtz(-f)
naphthalene	−383.352 408	−383.431 488	−383.456 429	−383.459 031
indole	−361.464 518	−361.544 528	−361.567 645	−361.571 225
2,3-benzofuran	−381.283 645	−381.366 543	−381.393 913	−381.397 120
C1	−722.933 120	−723.092 393	−723.137 770	−723.143 287
C1-2	−722.930 823	−723.090 325	−723.135 090	−723.141 397
C2	−762.564 629	−762.730 224	−762.783 464	−762.789 426
C2-2	−762.568 533	−762.734 056	−762.787 725	−762.793 532
T2	−766.706 402	−766.864 341	−766.913 209	−766.920 954
PD2	−766.699 950	−766.857 523	−766.905 773	−766.914 207
C	−766.700 601	−766.858 002	−766.906 547	−766.914 286
PD1	−766.700 876	−766.858 443	−766.906 794	−766.910 314
T1	−766.705 402	−766.860 831	−766.911 905	−766.917 088

TABLE 2: LMP2 Energies (hartree) of Studied Molecules and Their van der Waals Complexes Calculated at LM2/6-31G* Geometries

molecule	6-31G*	6-311G**	cc-pvtz(-f)	aug-cc-pvtz(-f)
naphthalene	−384.567 942	−384.750 734	−384.857 838	−384.873 507
indole	−362.602 137	−362.776 025	−362.877 679	−362.893 487
2,3-benzofuran	−382.434 555	−382.612 765	−382.722 878	−382.738 455
C1	−725.212 448	−725.560 142	−725.763 910	−725.796 381
C1-2	−725.213 965	−725.562 076	−725.766 432	−725.799 142
C2	−764.873 284	−765.230 291	−765.451 657	−765.484 815
C2-2	−764.873 712	−765.230 026	−765.450 742	−765.482 605
T2	−769.140 429	−769.506 339	−769.721 021	−769.753 327
PD2	−769.140 138	−769.506 783	−769.723 018	−769.759 318
C	−769.140 523	−769.507 002	−769.723 480	−769.757 751
PD1	−769.1401 17	−769.506 754	−769.722 751	−769.755 440
T1	−769.140 002	−769.503 742	−769.720 759	−769.749 591

TABLE 3: SCF Binding Energies (kcal/mol) of Studied van der Waals Complexes Calculated at LMP2/6-31G* Geometries

molecule	6-31G*	6-311G*	cc-pvtz(-f)	aug-cc-pvtz(-f)
C1	−1.45 (2.56)[a]	−1.30 (−2.09)	−1.31 (−1.56)	−0.67 (−0.53)
C1-2	0.32 (−1.12)	0.02 (−0.80)	0.19 (0.13)	0.42 (0.66)
C2	3.60 (−1.67)	3.19 (1.80)	3.17 (1.98)	3.38 (3.02)
C2-2	0.11 (−0.78)	0.17 (−0.61)	0.28 (0.06)	0.51 (0.44)
T2	−0.03 (−1.00)	−0.04 (−0.86)	0.06 (−0.22)	−0.18 (−0.59)
PD2	5.59 (3.05)	4.98 (3.42)	4.77 (4.45)	4.56 (4.86)
C	5.45 (2.64)	4.81 (3.12)	4.58 (3.96)	4.44 (4.63)
PD1	5.16 (2.47)	4.16 (2.84)	4.41 (3.81)	4.12 (4.22)
T1	0.73 (−0.24)	0.65 (−0.03)	0.71 (0.59)	0.57 (0.61)

[a] BSSE uncorrected values.

TABLE 4: LMP2 Binding Energies (kcal/mol) of Studied van der Waals Complexes Calculated at LMP2/6-31G* Geometries

molecule	6-31G*	6-311G**	cc-pvtz(-f)	aug-cc-pvtz(-f)
C1	−4.02 (−5.13)[a]	−4.29 (−5.08)	−5.12 (−5.37)	−6.04 (−5.90)
C1-2	−4.64 (−6.08)	−5.47 (−6.29)	−6.89 (−6.95)	−7.77 (−7.63)
C2	−0.69 (−2.62)	−1.6 (−2.99)	−2.51 (−3.70)	−4.60 (−4.96)
C2-2	−2.00 (−2.89)	−2.10 (−2.82)	−2.91 (−3.13)	−3.64 (−3.57)
T2	−1.88 (−2.85)	−2.24 (−3.06)	−3.07 (−3.35)	−3.55 (−3.96)
PD2	−0.13 (−2.67)	−1.78 (−3.34)	−4.29 (−4.61)	−8.02 (−7.72)
C	0.15 (−2.66)	−1.78 (−3.47)	−4.28 (−4.90)	−6.93 (−6.74)
PD1	0.03 (−2.66)	−2.0 (−3.32)	−3.84 (−4.44)	−5.38 (−5.28)
T1	−1.44 (−2.41)	−2.1 (−2.78)	−3.06 (−3.18)	−3.76 (−3.72)

[a] BSSE uncorrected values.

of the **C1** complex is the correlation energy as can be seen from the binding energy comparison at the SCF and LMP2 levels of theory (Tables 3 and 4). Thus, the calculations using the largest aug-cc-pvtz(-f) basis set show that SCF binding energy for **C1** complex is only −0.67 kcal/mol, while LMP2 binding energy is −6.04 kcal/mol.

The **C1-2** complex also presents evidences for π−hydrogen bond formation reflecting in pyramidalzation of nitrogen atoms of indole molecules. Unlike **C1,** where one indole molecule was a donor and another was an acceptor, in the **C1-2** complex each N−H bond of the pyrrole moiety participates in formation of π−hydrogen bonds with the benzene fragment of another indole molecule. The nitrogen lone pair in free indole is a pure p one while in the **C1-2** complex s character of the nitrogen lone pair increases from 0 to 2%. This causes the angle between the N−H bond and indole plane to becomes about 168° instead of 180° in the free indole molecule. The N−H bond length slightly increases to 1.013−1.014 Å compared to 1.011 Å for the indole molecule. These changes are less pronounced compared to the case for the **C1** complex due to looser complex structure. These geometrical changes indicate that the N−H π bond can be described in terms of $\pi-\sigma^*$ interactions.

TABLE 5: ΔE_{corr} Stabilization Energies (kcal/mol) of Studied Complexes at LMP2/6-31G* Geometries[a]

molecule	6-31G*	6-311G**	cc-pvtz(-f)	aug-cc-pvtz(-f)
C1	−2.57	−2.99	−3.81	−5.37
C1-2	−4.96	−5.49	−7.08	−8.29
C2	−4.29	−4.79	−5.68	−7.98
C2-2	−2.11	−2.21	−3.19	−4.01
T2	−1.85	−2.2	−3.13	−3.37
PD2	−5.72	−6.76	−9.06	−12.6
C	−5.30	−6.59	−8.86	−11.4
PD1	−5.13	−6.16	−8.25	−9.50
T1	−2.17	−2.75	−3.77	−4.33

ΔE_{corr} is defined as $[E_{AB}^{(LMP2)} - (E_A^{(LMP2)} - E_B^{(LMP2)})] - [E_{AB}^{(SCF)} - (E_A^{(SCF)} - E_B^{(SCF)})]$, where $E^{(SCF)}$ and $E^{(LMP2)}$ are SCF and LMP2 level energies of molecules A and B and molecular complex AB, respectively.

TABLE 6: MP2/6-31G* NBO Charges on Molecules in T-Shaped Complexes Perpendicular to Other Molecular Planes

complex	NBO molecular charge	complex	NBO molecular charge
C1	0.009	**T1**	0.005
C2-2	0.006	**T2**	0.005

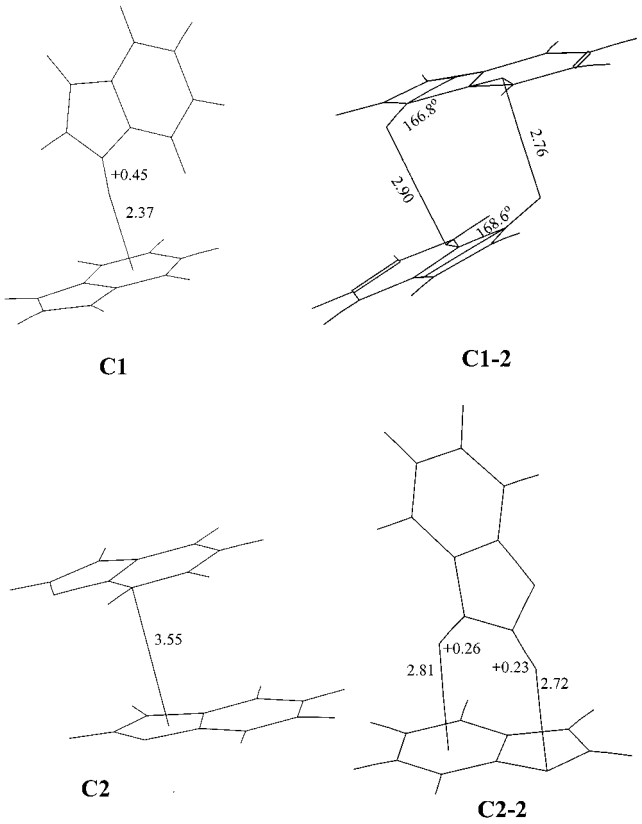

Figure 3. LMP2/6-31G*-optimized geometries of indole (**C1** and **C1-2**) and 2,3-benzofuran complexes (**C2** and **C2-2**).

When BSSE correction is taken into account, the binding energies are positive at SCF level for **C1-2,** while LMP2 correction shows that **C1-2** is more stable compared to **C1** at any level of theory reflecting greater correlation stabilization of the **C1-2** complex. The explanation of greater stability of **C1-2** compared to **C1** is similar to one given for stabilization of the **PD** and **C** naphthalene complexes compared to the **T** ones taking into account that the major contribution to the stabilization of indole complexes is the correlation stabilization.

2,3-Benzofuran Complexes. Figure 3 shows two lowest energy structures, the parallel (**C2**) and T-shaped (**C2-2**) ones found for the 2,3-benzofuran dimers. Similar to indole and naphthalene complexes, the T-shaped dimer (**C2-2**) is more stable at the SCF level compared to the parallel one (**C2**). Again, this can be attributed to C−H−π interactions that are confirmed by the charge transfer from one molecule to another (Table 6). The degree of charge transfer correlates with positive charge at the acceptor hydrogen atoms of monomers. Thus, the charge transfer is the greatest for indole complex and lowest for the naphthalene ones (Table 6), while NBO charges (MP2/6-31G* level) (Figures 2 and 3) at acceptor protons decrease from pyrrole to naphthalene. This finding is in accordance with the existence of X−H−π hydrogen bonds in T-shaped dimers of studied molecules. In the case of the **C2-2** dimer there are two nonequivalent protons H5 and H4 interacting with another 2,3-benzofuran molecule. While H4, similarly to indole and naphthalene complexes, interacts with π cloud of another molecule ($\pi-\sigma^*$ interaction), H5 participates in a p−σ^* interaction with the lone pair of an oxygen atom. This kind of bonding has been described earlier for a water−benzene complex, where benzene hydrogen interacts with the lone electron pair of water oxygen.[26] Slight geometrical changes occurring on complexation are also helpful to identify these weak interactions. Thus, C3−C4−H4 and O−C5−H5 angles increase from 127.9 and 114.8° to 128.1 and 115.1°, respectively; moreover the C4−H4 bond length becomes 0.001 Å longer.

TABLE 7: Kitaura−Morokuma Analysis of Molecular Complex Interaction Energies at the HF/6-31G* Level of Theory with the Unit of Each Energy Component in kcal/mol

complex	ES[a]	EX[b]	PL[c]	CT[d]	E[e]
C1	−3.59	3.05	−0.64	−1.53	−2.75
C1-2	−4.26	5.12	−0.83	−1.97	−1.91
C2	−0.01	3.04	−0.18	−1.61	1.34
C2-2	−1.61	2.00	−0.16	−1.22	−0.95
PD2	0.88	3.82	−0.26	−1.93	2.66
T2	−1.17	1.38	−0.17	−1.00	−0.95

[a] Electrostatic interaction. [b] Exchange repulsion. [c] Polarization interaction. [d] Charge-transfer interaction. [e] Total interaction energy.

The Kitaura−Morocuma analysis has been used[27] for SCF binding energy partition to understand the interaction energy differences between the parallel and T-shape complexes at the SCF level. The calculations were carried out using the GAMESS suite of programs at the LMP2/6-31G*-optimized geometry using the 6-31G* basis set. The results are shown in Table 7. As can be seen, the electrostatic and exchange interactions are responsible for the lower SCF energy of T-shape complexes compared to parallel ones. As can be seen from Table 7, in all parallel-oriented complexes the exchange interactions are more repulsive compared to T-shaped ones. Since the exchange interactions represent the short-range repulsion due to the overlap of electron distribution of one monomer with that of the other monomer, therefore, more positive exchange interactions found for parallel complexes reflect stronger overlap of π-electron clouds of monomers in parallel complexes. In a similar way, the electrostatic forces are less attractive for parallel complexes with the exception of the **C1-2** indole complex. As one could expect, the electrostatic interactions become stronger with polarity of X−H bonds in molecules increasing from naphthalene to indole complexes where they represent the most important attractive forces at the SCF level due to the strong dipole moment of the N−H bond.

Conclusions

The local MP2 method was found to be very useful for studying weak intermolecular complexes due to reduced BSSE (almost imperceptible at the aug-cc-pvtz(-f) level) as well as the possibility to use large basis sets for binding energy analysis for relatively large intermolecular complexes. The calculations show that the major contribution to the stabilization energy of studied complexes is the correlation stabilization, even in the case of indole dimers where the electrostatic interactions are the most significant. 2,3-Benzofuran and indole dimers definitely show the presence of X−H−π hydrogen bond as follows from the geometry changes and the charge transfer on complex formation. Naphthalene complexes do not present any perceptible geometric changes evidencing C−H−π hydrogen bond formation; however, they show a charge transfer similar to that observed for indole and 2,3-benzofuran complexes which can be attributed to weak C−H−π interaction.

The relative stability of molecular dimers shows strong dependence on the basis set size. Thus, for naphthalene and 2,3-benzofuran dimers, smaller basis sets predict T-shaped complexes to be more stable, while at the LMP2/aug-cc-pvtz(-f) level the most stable dimers are parallel in all cases. This is explained by the fact that T-shaped complexes are more stable at the SCF level compared to parallel ones due to stronger

electrostatic attraction and weaker exchange repulsion, while the parallel dimers show stronger correlation stabilization. Due to the faster energy convergence with the basis set size at the SCF level compared to the MP2 one, the use of small basis sets favors the stability of T-shaped dimers, while the use of larger basis sets clearly shows the parallel dimers to be most stable due to correlation stabilization.

Acknowledgment. This work was supported by Grants NC-204 and 33631E from the CONACyT.

References and Notes

(1) *Molecular Interactions. From van der Waals to Strongly Bound Complexes*; Scheiner, S., Ed.; Wiley: Chichester, U.K., 1997.
(2) Hobza, P.; Zahradanik, R. *Intermolecular Complexes*; Academia: Prague, 1988.
(3) Stone, A. J. *The Theory of Intermolecular Forces*; Clarendon Press:
(4) Oxford, U.K., 1996.
(5) Desiraju, G. R.; Steiner, T. *Weak Hydrogen Bond*: *In Structural*
(6) *Chemistry and Biology*; Oxford: New York, 1999.
(7) Nishio, M.; Hirota, M.; Umezawa, Y. *The CH-π Interaction*; Wiley-VCH: New York, 1998.
(8) Kaplan, I. G. *Molecular Interactions*; Elsevier: Amsterdam, 1986.
(9) Janda, K. C.; Hemminger, J. C.; Winn, J. S.; Novick, S. E.; Harris, S. J.; Klemperer, W. *J. Chem. Phys*. **1975**, *63*, 1419.
(10) Steed, J. M.; Dixon, T. A.; Klemperer, W. *J. Chem. Phys*. **1979**, *70*, 4940.
(11) Hobza, P.; Selzle H. L.; Schlag, E. W. *J. Phys. Chem*. **1996**, *100*, 18790.
(12) Syage, J. A.; Wessel, J. E. *J. Chem. Phys*. **1988**, *89*, 5962.
(13) Chakraborty, T.; Lim, E. C. J. *Phys. Chem*. **1993**, *97*, 11151.
(14) Gonzalez, C.; Lim E. C. *J. Phys. Chem. A* **2000**, *104*, 2953.
(15) Gonzalez, C.; Lim, E. C. *J. Phys. Chem*. *A* **1999**, *103*, 1437.
(16) Park, H.; Lee, S. *Chem. Phys Lett*. **1999**, *301*, 487.
(17) Møller, C.; Plesset, M. S. *Phys. Rev*. **1934**, *46*, 618.
(18) Zaremba, E.; Kohn, W. *Phys. Rev*. **1976**, *B13*, 2278; **1977**, *B15*, 1769.
(19) Saebo, S.; Tong, W.; Pulay, P. *J. Chem. Phys*. **1993**, *98*, 2170.
(20) Schutz, M.; Rauhut, G.; Werner, H.-J. *J. Phys. Chem. A* **1998**, *102*, 5997.
(21) Jaguar 4.1, Schrodinger, Inc., Portland, OR, 2000.
(22) Boys, S. F.; Bernardi, F. *Mol. Phys*. **1970**, *19*, 553.
(23) Frisch, M. J.; Trucks, G. W.; Schlegel, H. B.; Scuseria, G. E.; Robb, M. A.; Cheeseman, J. R.; Zakrzewski, V. G.; J. Montgomery, A.; Stratmann, Jr., R. E.; Burant, J. C.; Dapprich, S.; Millam, J. M.; Daniels, A. D.; Kudin, K. N.; Strain, M. C.; Farkas, O.; Tomasi, J.; Barone, V.; Cossi, M.; Cammi, R.; Mennucci, B.; Pomelli, C.; Adamo, C.; Clifford, S.; Ochterski, J.; Petersson, G. A.; Ayala, P. Y.; Cui, Q.; Morokuma, K.; Malick, D. K.; Rabuck, A. D.; Raghavachari, K.; Foresman, J. B.; Cioslowski, J.; Ortiz, J. V.; Baboul, A. G.; Stefanov, B. B.; Liu, G.; Liashenko, A.; Piskorz, P.; Komaromi, I.; Gomperts, R.; Martin, R. L.; Fox, D. J.; Keith, T.; Al-Laham, M. A.; Peng, C. Y.; Nanayakkara, A.; Challacombe, M.; Gill, P. M. W.; Johnson, B.; Chen, W.; Wong, M. W.; Andres, J. L.; Gonzalez, C.; Head-Gordon, M.; Replogle, E. S.; Pople, J. A. *Gaussian 98*, *Revision A.9*; Gaussian, Inc.: Pittsburgh, PA, 1998.
(24) Schmidt, M. W.; Baldridge, K. K.; Boatz, J. A.; Elbert, S. T.; Gordon, M. S.; Jensen, J. H.; Koseki, S.; Matsunaga, N.; Nguyen, K. A.; Su, S.; Windus, T. L.; Dupuis, M.; Montgomery, J. A. *J. Comput. Chem*. **1993**, *14*, 1347.
(25) Kaplan, I. G.; Roszak, S.; Leszczynsky, J. *J. Chem Phys*. **2000**, *113*, 6245.
(26) Tarakeshwar, P.; Choi, H. S.; and Kim, K. S. *J. Am. Chem. Soc*. **2001**, *123*, 3323.
(27) Scheiner, S. *Hydrogen Bonding*: *A Theoretical Perspective*; University Press: Oxford, U.K., 1997.
(28) Novoa, J.; Mota, F. *Chem. Phys. Lett*. **2000,** *318*, 345.
(29) Kitaura, K.; Morokuma, K. *Int. J. Quantum Chem*. **1976**, *10*, 325.